Inorg. Chem. 1983, 22, 1038-1048

Contribution from the Department of Chemistry,
Northwestern University, Evanston, Illinois 60201

Reversible Formation of $Pt_2(\mu\text{-H})_2H(PEt_3)_4^+$ and $Pt_2(\mu\text{-H})H_2(PEt_3)_4^+$ from the Cis and Trans Isomers of Dihydrobis(triethylphosphine)platinum(II)

RALPH S. PAONESSA and WILLIAM C. TROGLER*

Received June 8, 1982

Irradiation of $Pt(C_2O_4)L_2$, where L = $P(C_2H_5)_3$, in CH_3CN solvent under a hydrogen atmosphere produces $[Pt_2(\mu\text{-H})_2HL_4][O_2CH]$, **1**$[O_2CH]$, and CO_2. Dimer **1** can also be prepared by the condensation reaction between PtH_2L_2 (a 90:10 trans:cis equilibrium mixture) and $PtH(S)L_2^+$, where S = a solvent such as acetone. When PtD_2L_2 is used in the reaction, deuterium is only incorporated into the bridging positions. Analyses of the spin and isotopic distribution patterns in the ^{31}P, ^1H, and ^{195}Pt NMR spectra establish a solution geometry for **1** based on a *cis*-PtH_2L_2 molecule bound to the $PtHL_2^+$ fragment. The solution chemistry of **1** depends dramatically on the counterion. Basic anions X = I^-, OCH_3^-, and O_2CH^- generate small equilibrium concentrations of PtH_2L_2, $PtHXL_2$, and $[PtH(S)L_2]X$. For example, **1**$[O_2CH]$ reacts completely in the presence of C_2H_4 to yield $Pt(C_2H_4)L_2$ whereas **1**$[B(C_6H_5)_4]$ exhibits no such reactivity. Complex **1** efficiently catalyzes the decomposition of formic acid at 25 °C; however, formate ion must be added in excess to promote the reaction. Monomers appear to be the active catalysts. The species **1**[OH] formed by the addition of H_2O to PtH_2L_2 also catalyzes the hydration of acetonitrile to acetamide. A symmetrical isomer, $Pt_2(\mu\text{-H})H_2L_4^+$ (**2**), of dimer **1** can be generated by the UV photolysis of $Pt(C_2O_4)L_2$ in methanol. It appears that the initially formed *trans*-$PtH(OCH_3)L_2$ complex undergoes β-hydride abstraction to stereoselectively yield *trans*-PtH_2L_2. This species is trapped by *trans*-$PtH(OCH_3)L_2$ or [*trans*-$PtH(S)L_2][CH_3O]$ to form **2** before isomerization to *cis*-PtH_2L_2 (and thereby **1**) takes place. Dimer **2** is thermodynamically unstable with respect to **1**, and bases such as pyridine or I^- catalyze the isomerization. The relationship between the structures, fluxionality, and reactivity properties of **1**, **2**, and related dinuclear hydrido complexes is discussed. Lack of facile exchange between bridging and terminal hydrides in **1** and **2** is attributed to the trans disposition of terminal hydrogen to the bridging hydrogens.

Introduction

All cationic dimers of the formula $Pt_2H_3L_4^+$, where L is a tertiary phosphine ligand, contain two phosphine ligands per platinum but differ in geometry, number of bridging hydride ligands, and fluxional behavior.[1-4] In some closely related species, one or two terminal hydride ligands have been replaced by alkyl or aryl groups.[5,6] The compound $Pt_2(\mu\text{-H})H_2(\mu\text{-dppm})_2^+$ adopts an A-frame geometry in which the phosphorus and platinum atoms are roughly coplanar,[1] while species such as $Pt_2(\mu\text{-H})H_2(dbpp)_2^+$ (dbpp = $(t\text{-Bu})_2P(CH_2)_3P(t\text{-Bu})_2$) and $Pt_2Ph(\mu\text{-H})H(PEt_3)_4^+$ were shown by diffraction studies to contain approximately orthogonal PtP_2 coordination planes.[3,5,7] Dimers that have bis(phosphine) ligands on each platinum, $Pt_2(\mu\text{-H})H_2(bisphos)_2^+$, undergo rapid intramolecular exchange of terminal and bridging hydride ligands,[2,3] but other dimers do not.[1,4,5] In addition to those species that possess a single bridging hydride ligand, examples of doubly hydride-bridged compounds, $Pt_2(\mu\text{-H})_2HL_4^+$ (L = PPh_3, $P(c\text{-Hx})_3$, PEt_3), are known.[4] In a broader sense these dimers belong to a general class of 30-electron transition-metal dimers containing only phosphorus and hydride ligands. Included in this group are compounds such as $Ni_2(\mu\text{-H})_2(bisphos)_2$,[8] $Rh_2(\mu\text{-H})_3HL_3$ (L = $P(O\text{-}i\text{-Pr})_3$, $P(i\text{-Pr})_3$),[9a] $Rh_2(\mu\text{-H})_2H_2\{P[N(CH_3)_2]_3\}_4$[9b] $Ir_2(\mu\text{-H})_3H_2(PPh_3)_4^+$,[10] $Re_2(\mu\text{-H})_4H_4(PEt_2Ph)_4$,[11a] $Re_2(\mu\text{-H})_3H_3(PMe_2Ph)_5$,[11b] $Re_2(\mu\text{-H})_3H_2(PMe_2Ph)_4[P(OCH_2)_3CEt]_2^+$,[11c] $Re_2(\mu\text{-H})_3H(PMe_2Ph)_4[P(OCH_2)_3CEt]_2$,[11c] and $Fe_2(\mu\text{-H})_3(P_3)_2^+$ (P_3 = 1,1,1-tris((diphenylphosphino)methyl)ethane).[11d] Surprisingly little is known about the mechanisms by which these dimers form.

While studying the photochemistry of platinum(II) oxalate compounds[12] and the chemistry of sterically unhindered cis and trans dihydrides of platinum(II),[13] we encountered two isomeric dimers of the formula $Pt_2H_3(PEt_3)_4^+$, having one or two bridging hydride ligands. These dimers appeared to form from monomeric platinum(II) species, and an equilibrium between monomers and dimers could be established. A preliminary communication of some of these results has appeared.[13b] Our studies further lead to the conclusions that these dimers form by the binding of *cis*- and *trans*-$PtH_2(PEt_3)_2$ to a *trans*-$PtH(PEt_3)_2^+$ fragment and that the structures of all members of this class of platinum dimers can be idealized as the union of two square-planar platinum(II) centers that share one or two bridging hydride ligands.

Results

Formation of $Pt_2(\mu\text{-H})_2H(PEt_3)_4^+$ (1) and $Pt_2(\mu\text{-H})H_2(PEt_3)_4^+$ (2). Ultraviolet irradiation of the oxalate complex $Pt(C_2O_4)L_2$ (L = PEt_3) in acetonitrile under 1 atm of hydrogen produces $1^+HCO_2^-$ and free carbon dioxide. The structure shown for **1** is deduced from NMR and IR spectral data (see below). The signal for formate hydrogen in the ^1H NMR

---

(1) Brown, H. P.; Puddephatt, R. J.; Rashidi, M.; Seddon, K. R. *J. Chem. Soc., Dalton Trans.* **1978**, 516-522.

(2) Minghetti, G.; Banditelli, G.; Bandini, A. L. *J. Organomet. Chem.* **1977**, *139*, C80-C82.

(3) Tulip, T. H.; Yamagata, T.; Yoshida, T.; Wilson, R. D.; Ibers, J. A.; Otsuka, S. *Inorg. Chem.* **1979**, *18*, 2239-2250.

(4) (a) Bracher, G.; Grove, D. M.; Pregosin, P. S.; Venanzi, L. M. *Angew. Chem., Int. Ed. Engl.* **1979**, *18*, 155-156. (b) Venanzi, L. M. *Coord. Chem. Rev.* **1982**, *43*, 251-274.

(5) Bracher, G.; Grove, D. M.; Venanzi, L. M.; Bachechi, F.; Mura, P.; Zambonelli, L. *Angew. Chem., Int. Ed. Engl.* **1978**, *17*, 778-779.

(6) Brown, M. P.; Cooper, S. J.; Frew, A. A.; Manojlovic-Muir, L.; Muir, K. W.; Puddephatt, R. J.; Thomson, M. A. *J. Organomet. Chem.* **1980**, *198*, C33-C35; *J. Chem. Soc., Dalton Trans.* **1982**, 299-305.

(7) Abbreviations used: Me = methyl, Et = ethyl, Ph = phenyl, *t*-Bu = *tert*-butyl, *n*-Bu = *n*-butyl, *i*-Pr = isopropyl, dppm = bis(diphenylphosphino)methane, bisphos = any chelating bis(phosphine) ligand, COD = cyclooctadiene, S = solvent, dppe = bis(diphenylphosphino)ethane.

(8) (a) Jolly, P. W.; Wilke, G. "The Organic Chemistry of Nickel"; Academic Press: New York, 1974; Vol. I, pp 144-145. (b) Fischer, K.; Jonas, K.; Misbach, P.; Stabba, R.; Wilke, G. *Angew. Chem., Int. Ed. Engl.* **1973**, *12*, 943-953. (c) Kruger, K. *Ibid.* **1972**, *11*, 387-392.

(9) (a) Sivak, A. J.; Muetterties, E. L. *J. Am. Chem. Soc.* **1979**, *101*, 4878-4887. Thorn, D. L.; Ibers, J. A. *Adv. Chem. Ser.* **1982**, *No. 196*, 117-133. (b) Meier, E. G.; Burch, R. R.; Muetterties, E. L.; Day, V. W. *Ibid.* **1982**, *104*, 2661-2663.

(10) Crabtree, R. H.; Felkin, H.; Morris, G. E.; King, T. J.; Richards, J. A. *J. Organomet. Chem.* **1976**, *113*, C7-C9.

(11) (a) Bau, R.; Carroll, W. E.; Teller, R. G.; Koetzle, T. F. *J. Am. Chem. Soc.* **1977**, *99*, 3872-3874. (b) Green, M. A.; Huffman, J. C.; Caulton, K. G. *Ibid.* **1981**, *103*, 695-696. (c) Green, M. A.; Huffman, J. C.; Caulton, K. G. *Ibid.* **1982**, *104*, 2319-2320. (d) Dapporto, P.; Midollini, S.; Sacconi, L. *Inorg. Chem.* **1975**, *14*, 1643-1650.

(12) Paonessa, R. S.; Trogler, W. C. *Organometallics* **1982**, *1*, 768-770.

(13) (a) Paonessa, R. S.; Trogler, W. C. *J. Am. Chem. Soc.* **1982**, *104*, 1138-1140. (b) Paonessa, R. S.; Trogler, W. C. *Ibid.* **1982**, *104*, 3529-3530.

0020-1669/83/1322-1038$01.50/0

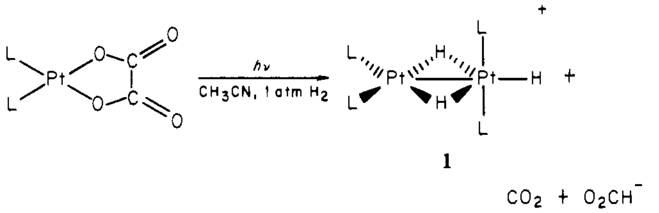

spectrum of $1^+HCO_2^-$ in CD_3CN is a sharp singlet at δ 8.54 and does not broaden between +30 and −50 °C. Metathesis with $LiBF_4$ or $NaBPh_4$ produces a precipitate of the alkali-metal formate salt. The compound $1^+BF_4^-$ was isolated from these solutions as an oil, while $1^+BPh_4^-$ could be prepared as air-stable yellow crystals.

Irradiation of $Pt(C_2O_4)L_2$ yields the 14-electron species PtL_2, accompanied by loss of 2 equiv of carbon dioxide.[12] Since sterically hindered $Pt(PR_3)_2$ complexes are known to oxidatively add H_2,[14] we investigated the possibility that PtH_2L_2 (**3**) is an intermediate in the photochemical formation of $1^+HCO_2^-$. Cis and trans isomers of **3** readily interconvert, and the equilibrium constant $K_i = [cis\text{-}3]/[trans\text{-}3]$ increases from 0.03 in hydrocarbon solvents to 0.1–0.2 in polar solvents.[13a] When a solution of predominantly *trans*-**3** in toluene-d_8 is placed under 1 atm of carbon dioxide, an equilibrium mixture of *trans*-**3** and *trans*-(formato)hydrobis(triethylphosphine)-platinum(II) (**4**) forms (eq 1). A signal for **4** appears in the

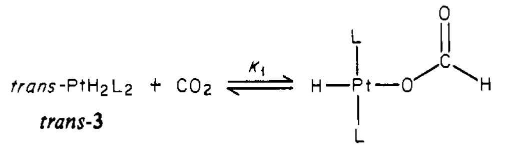

$$trans\text{-}PtH_2L_2 + CO_2 \overset{K_1}{\rightleftharpoons} H{-}PtL_2{-}O{-}C(=O)H \quad (1)$$

trans-**3** **4**

$^{31}P\{^1H\}$ NMR spectrum at δ 23.8 (s, $^1J_{PtP} = 2843$ Hz). Examination of the ^1H NMR spectrum of this solution reveals a signal for formate hydrogen (H_a) δ 9.36, d, broad, $^4J_{H_aH_b} = 4$ Hz, $^3J_{PtH_a} = 47$ Hz) and a signal for hydride (H_b δ −21.26, td, $^2J_{PH_b} = 16$ Hz, $^4J_{H_bH_a} = 4$ Hz, $^1J_{PtH_b} = 1176$ Hz) in a 1:1 intensity ratio. The ^{195}Pt coupling to the formate hydrogen resonance proves that formate ion is bound to platinum.[15a] From the $^{31}P\{^1H\}$ NMR spectra, the equilibrium constant K_1 is approximately 2 atm^{-1}. Complex **4** forms reversibly; bubbling nitrogen or hydrogen through a mixture of **3** and **4** leads to loss of CO_2 and conversion of **4** to **3**.

After 2 days at ambient temperature, or after prolonged UV irradiation, a mixture of *trans*-**3** and **4** in toluene-d_8 under 1 atm of carbon dioxide shows no sign of further reaction by ^{31}P NMR spectroscopy. Upon addition of an equal volume of a polar solvent such as acetonitrile, acetone, or tetrahydrofuran, $1^+HCO_2^-$ appears in the $^{31}P\{^1H\}$ NMR spectrum. The reaction between carbon dioxide and **3** in acetonitrile or acetone also rapidly produces $1^+HCO_2^-$. Complex **4** is not observed by $^{31}P\{^1H\}$ NMR spectroscopy in these polar solvents.

Complex **3** undergoes several oxidative-addition/reductive-elimination reactions, which appear to proceed via platinum(IV) intermediates.[13] Formic acid reacts with **3** in acetone-d_6 to produce a mixture of $1^+HCO_2^-$ and *trans*-$PtH(S)L_2^+$ (**5**) (S = acetone-d_6 or formic acid). The initial step in this reaction is probably protonation of **3** followed by reductive elimination of H_2 to give **5** (eq 2), or else oxidative

$$\underset{\mathbf{3}}{PtH_2L_2} + HCO_2H + S \rightarrow \underset{\mathbf{5}}{trans\text{-}PtH(S)L_2^+} + HCO_2^- + H_2 \quad (2)$$

$$\underset{\mathbf{3}}{PtH_2L_2} + HCO_2H \rightarrow \underset{\mathbf{4}}{trans\text{-}PtH(O_2CH)L_2} + H_2 \quad (3)$$

$$trans\text{-}PtH(O_2CH)L_2 + S \rightleftharpoons trans\text{-}PtH(S)L_2^+ + HCO_2^- \quad (4)$$

addition of HCO_2H and elimination of H_2 to yield **4** (eq 3). In either case, these species can interconvert via eq 4. Either of these complexes could react with **3** to produce **1**. Protic solvents such as methanol and water also react with **3** to cleanly form 1^+RO^- (R = CH_3, H). The reactions are slower than that with formic acid but reach completion within approximately 15 min at ambient temperature.

During studies of the formation of dimer **1**, we observed the transient formation of a second dimeric platinum species, **2**,

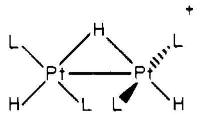

2

in the ^{31}P NMR spectra. This occurred in the reaction between **3** and formic acid or CO_2 in acetone. The early stages of reaction could be followed by mixing reagents in an NMR tube and transferring it to the probe of the spectrometer maintained at low temperature. This procedure showed similar amounts of **1** and **2** were produced initially in some reactions, but at longer times all the **2** that had formed was converted to **1**. Dimer **2** was, however, the exclusive product of another reaction. Ultraviolet irradiation of $Pt(C_2O_4)L_2$ in methanol at 25 °C yields a solution of *trans*-$PtH(OCH_3)L_2$ (**6**).[12] This complex is moderately stable in solution, but after several hours at 25 °C, or after 10 min at 60 °C, **6** converts completely to **2** in these solutions. Further standing at 25 °C for several hours does not result in any change in **2**, as evidenced by the $^{31}P\{^1H\}$ NMR spectrum, but heating causes slow isomerization to **1**. Attempts to isolate **2** from these solutions lead to partial or complete isomerization of **2** to **1**. Removal of the solvent produces a brown oil, which, when dissolved in acetone-d_6, is found to consist of **1** along with unidentified decomposition products. If the solutions are concentrated under vacuum, treated with $NaBPh_4$, and cooled to −20 °C for several hours, $2^+BPh_4^-$ contaminated with approximately 30–50% $1^+BPh_4^-$ precipitates.

Solutions of this mixture in acetone-d_6 are quite stable; dimer **2** does not convert to **1** after 30 min at 65 °C. Isomerization is slowly catalyzed by pyridine and rapidly catalyzed by iodide ion,[15b] either of which causes complete conversion of **2** to **1**. Thus **1** appears to be the thermodynamically preferred isomer.

NMR Spectra of $Pt_2(\mu\text{-}H)_2H(PEt_3)_4^+$ (1) and $Pt_2(\mu\text{-}H)H_2(PEt_3)_4^+$ (2). The presence of the readily observable spin-1/2 nuclei ^1H and ^{31}P (100% abundance) and ^{195}Pt (33.8% abundance) makes compounds **1** and **2** well suited to NMR study. Because these nuclei couple to one another, the spectra can be complex; however, detailed analysis of these couplings provides information about solution structures. We consider first the spectra of **1**. The labeling scheme for the discussion of the $^{31}P\{^1H\}$ NMR spectra is shown:

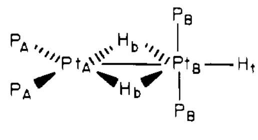

Note the two P_A atoms are magnetically inequivalent in the

---

(14) Yoshida, T.; Otsuka, S. *J. Am. Chem. Soc.* **1977**, *99*, 2134–2140.

(15) (a) The reaction between *trans*-$PtH_2[P(c\text{-}Hx)_3]_2$ and CO_2 produces an analogous formate complex, which was shown by X-ray diffraction to contain O-bonded formate. The close correspondence of the ^1H NMR parameters of this complex and those of **4** suggest an analogous structure for **4**. See: Immirzi, A.; Musco, A. *Inorg. Chim. Acta* **1977**, *22*, L35–L36. (b) If large amounts of I^- are added, then **1** reacts further (vide infra).

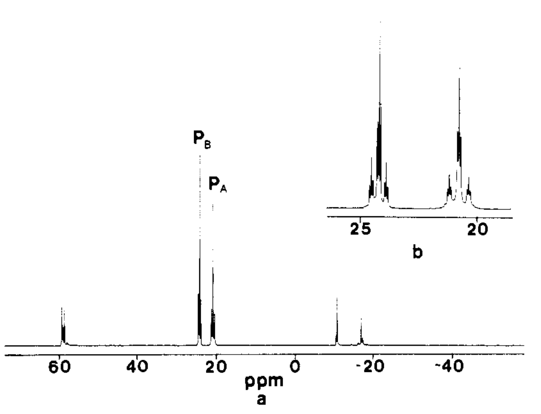

Figure 1. $^{31}P\{^1H\}$ NMR spectrum (36.3 MHz) of $1^+BPh_4^-$ in acetone-d_6 at 30 °C: (a) full spectrum; (b) expanded view of the central triplets, showing the long-range ($^2J_{PtP}$) satellites.

Chart I

isotopomer	% abundance	rel abundance
Pt_A, Pt_B; 1i	43.8	4
$^{195}Pt_A$, Pt_B; 1ii	22.4	2
Pt_A, $^{195}Pt_B$; 1iii	22.4	2
$^{195}Pt_A$, $^{195}Pt_B$; 1iv	11.4	1

^1H-coupled spectra but become magnetically equivalent when the spectra are ^1H decoupled. Values of coupling constants where the sign is not given represent absolute values; in cases where absolute or relative signs are known, they will be expressly given.

The dimeric nature of **1** was apparent from the $^{31}P\{^1H\}$ NMR spectrum (Figure 1). The strongest signals are a pair of 1:2:1 triplets, indicating the presence of two inequivalent pairs of mutually equivalent PEt_3 ligands (i.e., A_2B_2). Each triplet resonance is surrounded by a pair of symmetrically disposed satellites with large couplings ($^1J_{Pt_AP_A} = 2741$ Hz, $^1J_{Pt_BP_B} = 2540$ Hz), typical[16] of phosphorus bound to ^{195}Pt. In addition smaller couplings, indicative of coupling of each phosphorus to a distant ^{195}Pt atom, are also present ($^2J_{Pt_AP_B} = 23$ Hz, $^2J_{Pt_BP_A} = 30$ Hz). Resonances due to P_A and P_B were assigned by observing the ^{31}P NMR spectrum while decoupling only the triethylphosphine protons. When this was done, the P_A resonances were further split into doublets by the large coupling to the trans bridging hydrides. Dimer **1** should consist of four separate isotopomers distinguished by the presence or absence of ^{195}Pt at a given site; these are presented, along with their abundances based on a statistical distribution of ^{195}Pt, in Chart I. The observed $^{31}P\{^1H\}$ NMR spectrum of **1** (Figure 1) is the weighted sum of spectra due to these isotopomers. The two largest triplets arise from **1i**, which contains no ^{195}Pt. The presence of ^{195}Pt at Pt_A in **1ii** splits the P_A triplet into a doublet of triplets with the large doublet splitting $^1J_{Pt_AP_A}$ (Figure 1a); the P_B triplet is split into a doublet of triplets with the small doublet splitting $^2J_{Pt_AP_B}$ (Figure 1b). An analogous situation holds for **1iii**. Satellite signals due to **1ii** and **1iii** are one-fourth the intensity of the central signals due to **1v**; this agrees with the predicted abundance of isotopomers of **1**. Note that the contributions of **1i**–**1iii** have been analyzed completely in first-order terms. Further confirmation of the unsymmetrical dimeric nature of **1** comes from the $^{195}Pt\{^1H\}$ NMR spectrum (Figure 2a), which shows a separate set of resonances for Pt_A and Pt_B. Each resonance is split into a triplet by two phosphines directly bound to platinum; the long-range $^2J_{PtP}$ couplings are too small to be resolved. The $^{195}Pt\{^1H\}$ spectrum arising from **1iv** is second order (see below), but the value of $^1J_{Pt_APt_B} = 866$ Hz can be obtained directly, since it is the separation between the satellite lines surrounding each peak.

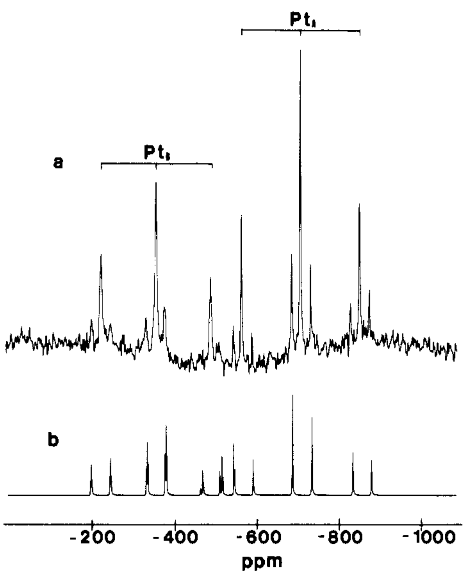

Figure 2. $^{195}Pt\{^1H\}$ NMR spectrum (19.2 MHz) of $1^+BPh_4^-$ in acetone-d_6 at 30 °C: (a) observed spectrum (the strongest signals are 1:2:1 triplets arising from Pt_A (δ −708) and Pt_B (δ −358), with each of these six lines being surrounded by a pair of satellite signals arising from isotopomer **1iv**); (b) computer simulation of the satellite signals arising from **1iv**.

The $^{31}P\{^1H\}$ and $^{195}Pt\{^1H\}$ NMR spectra of isotopomer **1iv** are second order,[17] corresponding to an A_2XYB_2 spin system. The outermost satellite signals of Figure 1a (also see supplementary figure 1) are the $^1J_{PtP}$ satellites from **1ii** and **1iii**, and the weak features are the signals of **1iv**. The chemical shift values and absolute values of the coupling constants that determine the spectrum of **1iv** are known directly from the first-order spectra of the isotopomers **1i**–**1iii**; only the signs of the coupling constants are undetermined. Using computer simulation, we systematically explored the effects of the signs of the J values on the spectral lines arising from **1iv**. The spectrum is invariant to the sign of $^1J_{Pt_APt_B}$, whose magnitude was established above; however, the relative signs of the $^1J_{PtP}$ and $^2J_{PtP}$ values have a pronounced effect on the simulated spectrum. Agreement between simulated and observed spectra is achieved when any three of these J values are of one sign, while the fourth is of opposite sign (supplementary figure 1). The sign of $^3J_{P_AP_B}$ has a minor but observable effect on certain lines, and comparison of simulated and experimental spectra indicates $^3J_{P_AP_B}$ is negative. We have also simulated the second-order $^{195}Pt\{^1H\}$ NMR spectrum of isotopomer **1iv**; this is shown in Figure 2b and corresponds to the satellite lines surrounding each of the six most intense resonances in Figure 2a. Note that the simulated intensity patterns agree well with those of the observed spectrum.

The 270-MHz ^1H NMR spectrum of the hydride region of **1** is complex (Figure 3a), but detailed analysis shows it to be consistent with the structure deduced for **1**. The labeling scheme

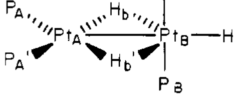

will be employed. (Note that since the phosphorus nuclei are not decoupled, both the P_A and H_b atoms are magnetically inequivalent.) The spectrum can be analyzed in three stages.

---

[16] Pregosin, P. S.; Kunz, R. W. *NMR: Basic Princ. Prog.* **1979**, *16*.

[17] Abraham, R. J. "The Analysis of High Resolution NMR Spectra"; Elsevier: New York, 1961.

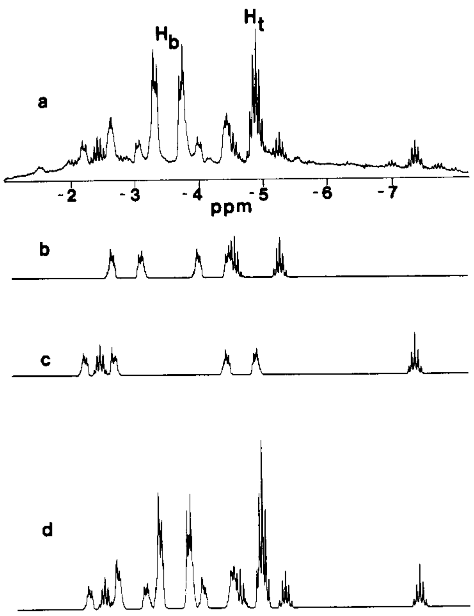

Figure 3. Hydride region of the ^1H NMR spectrum (270 MHz) of $1^+BPh_4^-$ (acetone-d_6, 30 °C): (a) observed spectrum; (b) simulated spectrum of isotopomer **1ii**; (c) simulated spectrum of isotopomer **1iii**; (d) simulated spectrum of the weighted sum of **1i** + **1ii** + **1iii**.

(1) The strongest multiplets are assigned to the hydrides in isotopomer **1i**, which has no ^{195}Pt splittings. These multiplets arise from all the first- and second-order couplings among the hydrogen and phosphorus nuclei and are shown in detail in supplementary figure 2a. The H_t resonance at δ −4.91 is an apparent quintet arising from coupling to two H_b nuclei and two P_B nuclei. The two H_b nuclei (δ −3.56) give rise to a complex overlapping group of multiplets, but the most prominent feature is the large doublet splitting caused by phosphines on Pt_A, which are trans to the H_b atoms.

(2) In the next stage of analysis, ^{195}Pt satellites, arising from **1ii** and **1iii**, are identified. These are simply "copies" of the central multiplets, and their separation is a direct measure of $^{195}Pt{-}H$ couplings. It is the observation of both direct and long-range couplings to H_t ($^1J_{Pt_BH_t} = 1316$ Hz, $^2J_{Pt_AH_t} = 191$ Hz) that identifies H_t as a terminal hydride. Conversely, the H_b hydrogens exhibit couplings that indicate they are each directly bound to both platinum atoms ($^1J_{PtH_b} = 592$ Hz, $^1J_{Pt'H_b} = 361$ Hz; Pt_A and Pt_B cannot be distinguished at this point). The values of $^1J_{PtH_b}$ and $^1J_{Pt'H_b}$ are smaller than those normally found for $^1J_{PtH}$ in mononuclear platinum(II) hydrides;[18] however, this is reasonable for bridging hydride ligands (see Discussion).

(3) Having identified terminal and bridging hydrides by analysis of the ^{195}Pt satellite patterns, we now examine the details of the parent hydride multiplets in terms of the proposed structure of **1**. The hydride spectrum of **1i**, with the triethylphosphine hydrogens ignored, arises from a second-order $XX'AA'BY_2$ spin system ($P_AP_A'H_bH_b'H_t(P_B)_2$). The spectrum will be truly second order if one or both of $J_{P_AP_A}$ or $J_{H_bH_b}$ is nonzero and first order otherwise.[17] Furthermore, the second-order part of the spectrum should, to a good approximation, be associated only with the *cis*-$Pt_A(P_A)_2(H_b)_2$ fragment, provided $J_{P_AP_A'}$ and $J_{H_bH_b'}$ are not too large; any couplings involving Pt_B, the two P_B atoms, or H_t will be nearly first order. The signal for H_t is an apparent 1:3:4:3:1 quintet; this arises from the splitting of H_t into a 1:2:1 triplet by two H_b nuclei ($^2J_{H_bH_t} = 13.68$ Hz) and splitting of these lines into 1:2:1 triplets by two P_B nuclei ($^2J_{P_BH_t} = 12.31$ Hz). Further examination of the H_b resonances reveals the presence of closely spaced triplets with the spacing 4.76 Hz; these could result from coupling of each H_b to two P_B nuclei, and hence we have $^2J_{P_BH_b} = 4.76$ Hz. There is no resolved coupling for $^3J_{P_AH_t}$. This is as far as we can proceed by considering only first-order couplings.

Chart II

isotopomer	% abundance	rel abundance
Pt, Pt; **2i**	43.8	4
^{195}Pt, Pt; **2ii**	44.8	4
^{195}Pt, ^{195}Pt; **2iii**	11.4	1

Second-order effects manifest themselves in the H_b multiplets. The H_b nuclei can be treated as part of a second-order $XX'AA'$ spin system, which are further split by the first-order couplings described above. The $XX'AA'$ spin system has been fully analyzed elsewhere.[17] When $J_{P_AP_A'} = J_{H_bH_b'} = 0$, the spectrum would be a 1:1:1:1 doublet of doublets (if couplings to H_t and P_B are ignored). If one or both of $J_{P_AP_A'}$ or $J_{H_bH_b'}$ is nonzero, a further splitting will appear in either the inner lines (if $^2J_{P_AH_b}{}^{cis}$ and $^2J_{P_AH_b'}{}^{trans}$ are of the same sign) or the outer lines (if $^2J_{P_AH_b}{}^{cis}$ and $^2J_{P_AH_b'}{}^{trans}$ are of opposite signs). The presence of unresolved broadening on the *outside* of each of the two major H_b multiplets suggests that the latter has occurred and that $^2J_{P_AH_t}{}^{cis}$ is sufficiently small that the outer lines partly overlap the inner lines. At this point computer simulation of the spectrum is employed, with the values of $^2J_{P_AP_A'}$, $^2J_{H_bH_b'}$, $^2J_{P_AHb'}{}^{cis}$ and $^2J_{P_AH_b'}{}^{trans}$ varied until a good fit is obtained. Because many of the lines were unresolved, we did not attempt a least-squares optimization of the coupling constants but instead sought a spectrum that visually matched the observed one.[19] The simulated spectrum thus obtained is shown in supplementary figure 2b, with the values $^2J_{P_AH_b}{}^{cis} = \pm 6.5$ Hz, $^2J_{P_AH_b'} = \mp 125$ Hz, $^2J_{P_AP_A'} = 10$ Hz, and $^2J_{H_bH_b'} = 5$ Hz, along with the other couplings disscussed above. Small changes in $^2J_{P_AP_A'}$ and $^2J_{H_bH_b'}$ produce subtle differences in the spectrum, and because of the degree to which multiplets overlap, these values are approximate. The important result is that the values indicate the *presence of a cis-*PtH_2P_2 *fragment connected via its hydride ligands to a second platinum atom.* For comparison, the coupling constants for *cis*-$PtH_2(PEt_3)_2$ are $^2J_{PH}{}^{cis} = \pm 24$ Hz and $^2J_{PH}{}^{trans} = \mp 172$ Hz.[13] Values of $^2J_{PP}{}^{cis}$ for platinum(II) complexes fall in the range 10–50 Hz and are negative, while values of $^2J_{PP}{}^{trans}$ are typically an order of magnitude larger and are positive.[11] Figure 3d shows the simulated spectrum for the weighted sum of **1i**–**1iii**. Because of the complexity and overlap in the spectrum, the minor contribution (10.4%) of **1iv** ($XX'AA'MNY_2B$ spectrum) was not simulated.

Both the IR and the ^1H NMR spectra of **2** indicate the presence of terminal and bridging hydrides, and an analysis of the ^1H NMR spectrum demonstrates the presence of one bridging and two equivalent terminal hydrides. The $^{31}P\{^1H\}$ NMR spectrum consists of a central singlet flanked by ^{195}Pt satellites in a pattern typical of the symmetrical dimers $[Pt(PR_3)_2X_n]_2$. Spectra of **2** arise from the three isotopomers given in Chart II. The labeling scheme

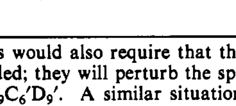

---

[18] Appleton, T. G.; Clark, H. C.; Manzer, L. E. *Coord. Chem. Rev.* **1973**, *10*, 335–422.

[19] An exact analysis would also require that the effect of the PEt_3 hydrogens be included; they will perturb the spin system by adding the components $C_6D_9C_6'D_9'$. A similar situation was encountered[20] for *cis*-$Pt(Me)_2(PMe_3)_2$. These couplings will not affect the major lines of the H_b resonances and do not alter the analysis presented here.

[20] Goodfellow, R. J.; Hardy, M. J.; Taylor, B. F. *J. Chem. Soc., Dalton Trans.* **1973**, 2450–2453.

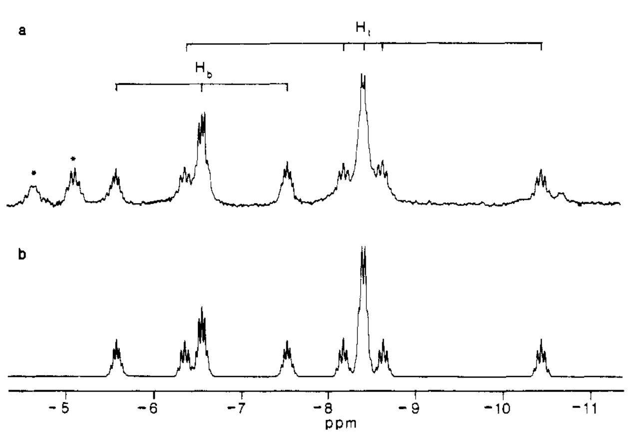

Figure 4. Hydride region of the ^1H NMR spectrum (270 MHz) of $2^+BPh_4^-$ (acetone-d_6, 30 °C): (a) observed spectrum (signals marked by an asterisk arise from $1^+BPh_4^-$); (b) simulated spectrum of the weighted sum of **2i** + **2ii**.

will be used. Examination of the $^{31}P\{^1H\}$ NMR spectrum of **2** reveals $^1J_{PtP} = 2574$ Hz and $^2J_{PtP'} = 18$ Hz; these values are obtained directly from the spacings between ^{195}Pt satellites that arise from isotopomer **2ii**. The total integrated intensity of these four satellite lines equals that of the central line of **2i**, in agreement with the expected isotopomer distribution. We have not been able to resolve P-P′ splitting in the signals of isotopomer **2ii**; therefore $^3J_{PP'} < 2$ Hz. Isotopomer **2iii** provides an $A_2XX'A_2'$ spin system, which has been analyzed previously[21] and discussed with respect to platinum dimers;[3] the most intense feature is a doublet of separation $N = |^1J_{PtP} + {}^2J_{PtP'}|$. This separation is 2556 Hz for **2**, and since values of $^1J_{PtP}$ are positive[22] and in this case the value is 2574 Hz, $^2J_{PtP'}$ must be −18 Hz. We have not been able to observe other lines assignable to isotopomer **2iii**, but they are expected to be weak.

The ^1H NMR spectrum of **2** (Figure 4a) contains a signal for two terminal hydrides as a multiplet at δ −8.41. Consistent with this assignment, we observe couplings to directly bound ^{195}Pt ($^1J_{PtH_t} = 1100$ Hz) and to distant ^{195}Pt ($^2J_{PtH_t'} = 122$ Hz). The bridging hydride multiplet at δ −6.57 is split into a 1:7.8:17.3:7.8:1 quintet by ^{195}Pt satellites, typical of nuclei that symmetrically bridge two equivalent platinum centers;[23] the spacing corresponds to the value $^1J_{PtH_b} = 529$ Hz. The detailed structure of each multiplet depends on couplings among the hydrogen, phosphorus, and platinum nuclei. The hydride spectrum of **2i** arises from an $AX_2BX_2'A'$ spin system ($H_tP_2H_bP_2'H_t'$), the satellites due to **2ii** are part of an $AMX_2BX_2'A'$ spin system (M = ^{195}Pt), and the spectrum due to **2iii** is from an $AMX_2BX_2'M'A'$ spin system; all are second-order. Measurement of the multiplet splittings provides the coupling constant values $^2J_{PH_t} = 12.2$ Hz, $^2J_{PH_b} = {}^2J_{P'H_b} = 8.55$ Hz, and $^2J_{H_tH_b} = 9.77$ Hz. The values of $^2J_{PH}$ are typical of those found for hydride cis to a phosphine, and the value of $^2J_{H_tH_b}$ is similar to that for **1**. Coupling corresponding to $^3J_{PH_t'}$ was not observed. A value for $^3J_{H_tH_t'}$ of about 10 Hz was found by comparison of observed and computer-simulated spectra of **2i** and **2ii**; the simulated spectrum is shown in Figure 4b. Note the interesting result that the ^{195}Pt satellites of H_t arising from **2ii** are not identical with the parent signal arising from **2i**. This is a manifestation of the differences between the respective second-order spin systems of **2i** and **2ii** (caused by the absence or presence of ^{195}Pt).

Solution Behavior of $Pt_2(\mu\text{-}H)_2H(PEt_3)_4^+$ (1). Several lines of evidence indicate that in solution the dimeric species 1^+X^- is in equilibrium with the monomeric precursors **3** and *trans*-$PtHXL_2$ and that the extent of this equilibrium varies with the nature of X^-. Addition of *n*-$Bu_4^+I^-$ to a solution of $1^+BPh_4^-$ establishes the equilibrium shown in eq 5. Counterions BPh_4^- and *n*-Bu_4N^+ are not shown, but it should be noted that their involvement in ion-pairing equilibria could affect the position of the equilibrium (see Discussion). Integration of the $^{31}P\{^1H\}$ NMR spectra of mixtures of $1^+BPh_4^-$ and *n*-$Bu_4N^+I^-$ in acetone-d_6 at 25 °C gives an approximate value for the equilibrium constant $K_5 = 0.15 \pm 0.1$. Lowering the temperature causes the equilibrium to shift to the left ($K_5 \approx 0.009$ at −30 °C). A plot of ln K_5 vs. $1/T$ for the range +30 to −30 °C is linear and gives the value $\Delta H = -7.4 \pm 2$ kcal mol^{-1}, which in turn yields $\Delta S = 21 \pm 6$ cal mol^{-1} K^{-1}. Significant broadening of the NMR signals occurs at 25 °C, and this broadening increases as the temperature or the concentration of I^- increases. Between 50 and 100 °C, this prevented the observation of signals.

$$\underset{\mathbf{1}}{Pt_2(\mu\text{-}H)_2HL_4^+} + I^- \overset{K_5}{\rightleftharpoons} \underset{\mathbf{3}}{PtH_2L_2} + trans\text{-}PtHIL_2 \quad (5)$$

Addition of a 200-fold excess of sodium methoxide to a solution of $1^+CH_3O^-$ in methanol does not produce detectable $^{31}P\{^1H\}$ NMR signals for the monomers **3** or **6**. The ability of CH_3O^- to react with 1^+ is, however, demonstrated by the decomposition of $1^+CH_3O^-$ (in the absence of excess $NaOCH_3$) to PtL_3 and platinum metal when the methanol solvent is removed under vacuum at 25 °C. The same decomposition products are observed when the solvent is removed from solutions of **3** or **6**.[13] In comparison, solutions of $1^+BPh_4^-$ or $1^+BF_4^-$ show no signs of decomposition upon removal of the solvent, and these species are indefinitely stable under vacuum. The ability of methoxide ion to react reversibly with 1^+, but the absence of observable concentrations of **3** and **6** in the presence of excess methoxide, suggests the equilibrium constant for eq 6 is less than ~10^{-3}.

$$\underset{\mathbf{1}}{Pt_2(\mu\text{-}H)_2HL_4^+} + CH_3O^- \overset{K_6}{\rightleftharpoons} \underset{\mathbf{3}}{PtH_2L_2} + \underset{\mathbf{6}}{trans\text{-}PtH(OCH_3)L_2} \quad (6)$$

Several experiments indicate $1^+HCO_2^-$ is also in equilibrium with its monomeric precursors, **3** and **4** (or **5**) (eq 7). As in the case of $1^+CH_3O^-$, the equilibrium must lie far to the left, since these monomers cannot be detected in the $^{31}P\{^1H\}$ NMR spectra of solutions of $1^+HCO_2^-$. Passing a stream of hydrogen through a solution of $1^+HCO_2^-$ at 25 °C for several hours slowly sweeps CO_2 from the system, and **1** reverts completely to **3**. Under vacuum, solutions of $1^+HCO_2^-$ decompose to a mixture of PtL_3 and platinum metal; as discussed above, these are the observed decomposition products of **3** under vacuum, and loss of CO_2 from **4** to yield **3** readily occurs. Further evidence of reversibility comes from the observation that a solution of $1^+HCO_2^-$ placed under an atmosphere of $^{13}CO_2$ rapidly forms $H^{13}CO_2^-$ (within 0.2 h at 25 °C), as seen from the appearance of ^{13}C satellites around the formate signal in the ^1H NMR spectrum. Incorporation of ^{13}C could occur by exchange of labeled and unlabeled carbon dioxide in the equilibrium between **3** and **4** (eq 1). When a solution of $1^+HCO_2^-$ is placed under 1 atm of ethylene, slow conversion over 2 days at 25 °C produces $Pt(C_2H_4)L_2$, presumably as in eq 8. Ethylene is known to react rapidly with **3** to form

$$\underset{\mathbf{1^+}}{Pt_2(\mu\text{-}H)_2HL_4^+} + HCO_2^- \overset{K_7}{\rightleftharpoons} \underset{\mathbf{3}}{PtH_2L_2} + \underset{\mathbf{4}}{PtH(O_2CH)L_2} \quad (7)$$

$$Pt_2(\mu\text{-}H)_2HL_4^+ + HCO_2^- + 2C_2H_4 \rightarrow 2Pt(C_2H_4)L_2 + 2H_2 + CO_2 \quad (8)$$

---

[21] (a) Harris, R. K. *Can. J. Chem.* **1964**, *42*, 2275–2281. (b) Harris, R. K.; Woodman, C. M. *Mol. Phys.* **1966**, 437–449.

[22] McFarlane, W. J. *J. Chem. Soc. A* **1967**, 1922–1923.

[23] Brown, M. P.; Puddephatt, R. J.; Rashidi, M.; Seddon, K. R. *J. Chem. Soc., Dalton Trans.* **1977**, 951–955.

Table I. $^{31}P\{^1H\}$ NMR Data for Cationic Platinum Dimers

	P_A			P_B					
dimer	$\delta(P_A)$[a]	$^1J_{Pt_AP_A}$, Hz	$^2J_{Pt_BP_A}$, Hz	$\delta(P_B)$[a]	$^1J_{Pt_BP_B}$, Hz	$^2J_{Pt_AP_B}$, Hz	$^3J_{P_AP_B}$, Hz	$^1J_{Pt_APt_B}$, Hz	ref
1[b]	20.8 t	+2741	±30	24.2 t	+2540	∓23	−2.9	866	this work
$Pt_2H(\mu\text{-}H)_2(PPh_3)_4^+$[c,e]	31.9 t	3008	42	26.6 t	2803	18		325	4
2[b]	19.9	+2574	−18				<2		this work
7[d,f]	19.0 t	2591	12	8.2 t	2629	13		366	5
9[d]	17.9	+2770	+16						1
10[b]	49.4	+3039	+168				6.8	840	3

[a] Central resonances are singlets unless otherwise noted; t = 1:2:1 triplet. [b] BPh_4^- counterion. [c] BF_4^- counterion. [d] PF_6^- counterion. [e] Same labeling scheme as for 1. [f] Terminal hydride is bound to Pt_A.

Scheme I. Proposed Equilibria in the Catalysis of $HCO_2H \rightarrow H_2 + CO_2$ ($L = PEt_3$; $S = HCO_2H$, $(CH_3)_2CO$, or CH_3OH)

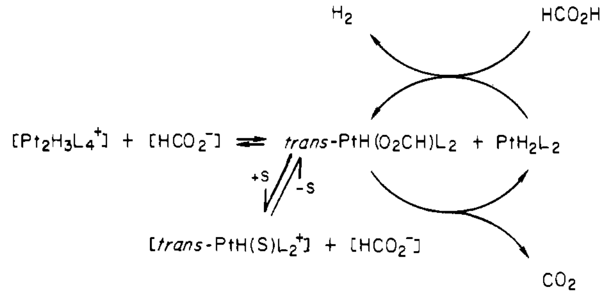

$Pt(C_2H_4)L_2$ and H_2.[13] Importantly, under identical conditions $1^+BPh_4^-$ did *not* react with ethylene, demonstrating the key role of formate ion in eq 8.

These observations suggest an interesting possibility for a catalytic system. A cycle for the catalytic decomposition of formic acid to hydrogen and carbon dioxide can be formed from eq 2–4 and the reverse of eq 1; the catalytically active species are proposed to be in equilibrium with 1^+ and HCO_2^- (eq 7). These reactions are assembled in Scheme I. In accord with this proposal, we find that $1^+BPh_4^-$, in the absence of added formate ion, is ineffective as a catalyst in solution for the decomposition of formic acid at 20 °C, but when a 200-fold excess of sodium formate is added, catalysis occurs. The turnover rate is 3.3 ± 0.5 mol of HCO_2H (mol of 3)$^{-1}$ h^{-1} at 20 °C. Several hundred turnovers were observed, throughout which time the solutions remain homogeneous and do not lose activity. When the catalysis is performed in methanol solutions of formic acid, only 1 can be detected by $^{31}P\{^1H\}$ NMR spectroscopy. If $1^+BPh_4^-$ is dissolved in a mixture of formic acid and acetone-d_6 (5:1 v/v), however, a mixture of 1 and 5 forms over several hours. These species also form when 3 is dissolved in formic acid. It is interesting that the counterion plays such an important role in the chemistry of 1. Intermediates such as those discussed above may be involved in the transfer hydrogenolysis of aryl bromides by sodium formate in the presence of $PdCl_2(PPh_3)_2$ catalyst.[24]

Hydration of acetonitrile to acetamide is catalyzed by 1^+OH^- at 25 °C (eq 9). The observation of this base-catalyzed

$$CH_3CN + H_2O \xrightarrow{[1^+OH^-]} CH_3C(O)NH_2 \qquad (9)$$

reaction supports the conclusion that hydroxide ion forms in the reaction of 3 and water (see above). Catalysis of nitrile hydration reactions by platinum(II) compounds, *trans*-$PtH(OH)(PR_3)_2$, and *trans*-$Pt(OH)R(PR'_3)_2$ has been described;[25,26] loss of hydroxide ion from mononuclear platinum(II) species was thought to be a key step in those reactions.

If one assumes dimer 1 forms by combination of the monomeric dihydride 3 with the fragment $PtHL_2^+$, the following question arises: which hydride ligands become bridging, and which become terminal? A deuterium-labeling experiment suggests the bridging hydrides of 1 are derived exclusively from *cis*-3, while the terminal hydride originates from the $PtHL_2^+$ fragment. When PtD_2L_2 and [*trans*-$PtH(NCCD_3)L_2$][BF_4] react in acetonitrile-d_3, [$Pt_2(\mu\text{-}D)_2HL_4$][BF_4] rapidly forms. The hydride portion of the ^1H NMR spectrum shows only a signal for the terminal hydride as a complex multiplet at δ −4.77, in precise agreement with the chemical shift of terminal hydride observed for $1^+BPh_4^-$ in this solvent. Extra splitting in the multiplet for 1-d_2 results from the two bridging deuterium atoms ($I = 1$). No proton resonances for hydrogen in the bridging position can be detected.

Discussion

Stereochemistry and Fluxional Behavior. Dimeric complexes 1 and 2 represent two distinct structural types within the class of hydride-bridged platinum(II) dimers of formula $[Pt_2H_nR_{3-n}(PR_3')_4][X]$, $n = 1$–3. It is informative to compare the structures of 1 to 2 with those of the other members of this series,[1,6] since the reported geometries serve as useful reference points in assigning structures. In addition, comparisons among the complexes reveal trends and classifications for their formation, geometries, NMR spectra, and fluxional behavior.

The dimer $Pt_2(\mu\text{-}H)HPh(PEt_2)_4^+$ (7) has been shown by

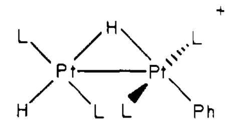

7

X-ray diffraction and NMR spectroscopy to consist essentially of two interlocking square-planar platinum(II) moieties whose coordination planes are inclined at a dihedral angle of 85° around the Pt–Pt vector.[5] The Pt–Pt separation of 3.09 Å indicates a weak metal–metal interaction. Since the hydride ligand is electronically similar to the σ-bound phenyl ligand in platinum(II) complexes, we propose the geometry of 2 can be modeled after that of 7. Similarities of the NMR parameters of 2 and 7, shown in Tables I and II, support this analogy. The essential features of the structure are the trans disposition of phosphine ligands on each platinum and the orthogonal orientation of the two coordination planes. The nature of the structure suggests a conceptually useful way of idealizing the geometry of these and related members of the series that contain a single bridging hydride ligand. These dimers can be considered formally to consist of a square-planar *trans*-

---

(24) Bar, R.; Sasson, Y.; Blum, J. *J. Mol. Catal.* **1982**, *16*, 175–180.

(25) Yoshida, T.; Matsuda, T.; Okano, T.; Kitani, T.; Otsuka, S. *J. Am. Chem. Soc.* **1979**, *101*, 2027–2038.

(26) Arnold, D. P.; Bennett, M. A. *J. Organomet. Chem.* **1980**, *199*, 119–135.

Table II. Hydride ^1H NMR Data for Cationic Platinum Dimers[a]

	terminal hydride				bridging hydride					
dimer	$\delta(H_t)$	$^1J_{PtH_t}$, Hz	$^2J_{PtH_t}$, Hz	$^2J_{PH_t}{}^{cis}$, Hz	$\delta(H_b)$	$^1J_{PtH_b}$, Hz	$^1J_{Pt'H_b}$, Hz	$^2J_{PH_b}{}^{cis}$, Hz	$^2J_{PH_b}{}^{trans}$, Hz	$^2J_{H_tH_b}$, Hz
1[b]	−4.91	1316	191	12.31	−3.56	592	361	±6.5	∓125	13.68
$Pt_2H(\mu\text{-}H)_2(PPh_3)_4^+$ [c]	−4.75	1197	226	25	−3.20	601	397	nr[f]	nr[f]	14
2[b]	−8.41	1100	122	12.2	−6.57	529		8.55		9.77
7[d]	−11.45	1148	108	nr	−9.46	~500	~500	nr		nr
9[d]	−6.86	1138	103	nr	−5.86	540				
10[b,g]										

[a] nr = not reported; see Table I for references. [b] BPh_4^- counterion. [c] BF_4^- counterion. [d] PF_6^- counterion. [e] Coupling to P_A. $^2J_{P_BH_t}{}^{cis} = 4.76$ Hz. [f] $^2J_{PH_b}{}^{cis} + {}^2J_{PH_b}{}^{trans} = 110$ Hz. [g] Rapid exchange of H_t and H_b: δ −5.89, $J_{PtH} = 395.7$ Hz, $J_{PH} = 37.9$ Hz.

PtL_2R^+ moiety in which the coordination site opposite R is occupied by the Pt–H bond of a *trans*-$PtHR'L_2$ molecule. To the extent the dimer is symmetric, the picture can be reversed; two "resonance structures" that result are shown in **8**. This description is, in fact, equivalent to the more conventional picture of a three-center–two-electron bond for the Pt(μ-H)Pt moiety since the orbitals used are the same.[27a] The conceptual value of the formalism diagrammed in **8** is that it retains the square-planar description of the idealized geometry at each platinum and it reflects how the dimers form and come apart (see below).

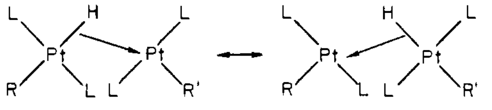

8

The precise position of the hydride ligands in **2** and **7** is a matter of conjecture. Both halves of **2** are equivalent in solution on the NMR time scale, and the terminal and bridging hydrides do not interchange on the NMR time scale. If one assumes the PtP_2 planes are not coplanar in **2**, then it is impossible to define a rigid structure in which the phosphine ligands are all chemically equivalent; the bridging hydride ligand lowers the symmetry. It is therefore likely that the structure of **2** in solution is nonrigid and that some degree of torsional motion around the Pt–Pt vector occurs. This is also required for **7**; two phosphine ligands bound to one platinum are chemically inequivalent in the solid-state structure but are chemically equivalent in solution.[5]

An alternate symmetrical structure that can be considered for **2** is the A-frame geometry deduced spectroscopically for $Pt_2(\mu\text{-}H)H_2(\mu\text{-dppm})_2^+$ (**9**)[1] and confirmed by X-ray diffraction for the closely related complex in which methyl groups replace the terminal hydride ligands.[6] This structure would in principle give rise in the ^{31}P NMR spectrum of **2** to an AA′A″A‴X pattern for the ^{195}Pt satellites[1] instead of the $A_2A_2'X$ pattern expected from the geometry we propose. Unfortunately, no $^3J_{PP'}$ coupling of any sort is resolved for **2**, and so this criterion cannot be applied. The A-frame geometry of **9** is imposed by the bridging dppm ligands; in the absence of this constraint, we believe **7** provides a better model of the geometry of **2** than does **9**.

A series of dimers $Pt_2H_3(bisphos)_2^+$, where bisphos represents any of a number of chelating bis(phosphine) ligands, have been prepared.[2,3] One member of this group, **10** (bisphos = $(t\text{-}Bu)_2P(CH_2)_3P(t\text{-}Bu)_2$), has been characterized by X-ray diffraction and exhibits an approximately symmetrical structure with one bridging and two terminal hydride ligands.[3] Although the structure was described in terms of a highly distorted trigonal-bipyramidal geometry at platinum (in which the Pt–Pt and Pt–(μ-H) bonds are taken to occupy separate coordination sites),[3] we will consider it here in the same structural framework presented above (i.e., idealized four-coordinate square-planar geometry at platinum). When it is viewed this way, **10** is the cis–cis analogue of **2** and **7**, which have trans–trans geometries at platinum. This cis orientation of phosphines is imposed by the chelating bisphos ligand. In **10**, the terminal hydride ligands occupy coordination sites cis to the Pt(μ-H)Pt bond, rather than trans to it as in **2** and **9**. Significantly, dimers of structure type **10** undergo rapid interchange of bridging and terminal hydride ligands on the NMR time scale even at low temperatures.[3] We suggest this facile interchange results from the cis disposition of terminal hydride to the Pt(μ-H)Pt bond.

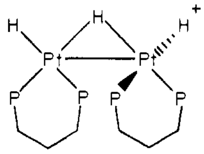

10

Dimer **1** possesses two bridging hydride ligands. No platinum analogues had been reported and characterized by X-ray diffraction.[27b] Fortunately, the amount of detail that is found in the NMR spectra of **1** allows one to deduce details of the solution structure with a high degree of confidence. Several constraints are imposed by the spectral data. The orthogonality of the two PtP_2 planes is indicated by the observation of simple A_2B_2 splitting of each phosphorus resonance into a 1:2:1 triplet. Significant deviation from orthogonality would product an AA′BB′ splitting, as seen for unsymmetrical A-frame dimers where the PtP_2 planes are constrained to be coplanar.[28] The equal coupling in the ^1H NMR spectrum between each P_B nucleus and the two H_b nuclei requires the P_B atoms to be located symmetrically above and below the *cis*-$Pt_A(H_b)_2(P_A)_2$ coordination plane. The presence of a *cis*-PtH_2P_2 moiety is indicated by the ^1H NMR spectrum and the selectively decoupled ^{31}P NMR spectrum. The interesting discovery that the long-range couplings $^2J_{Pt_AP_B}$ and $^2J_{Pt_BP_A}$ are of opposite sign seems reasonable, given the different orientation of P_A and P_B with respect to the Pt(μ-H)$_2$Pt pseudoplane.

---

[27] (a) The interaction diagrammed in **8** is based upon three σ orbitals: a vacant acceptor orbital on $PtRP_2^+$ and the two orbitals that form the occupied Pt–H bonding molecular orbital of $PtHR'L_2$. These three orbitals could equally well be described as coming together to form a three-center molecular orbital, populated by a pair of electrons. (b) After submitting this manuscript, we learned from Prof. L. M. Venanzi and co-workers that dimer **1** has been characterized by X-ray diffraction (see preceding paper).

[28] Brown, M. P.; Puddephatt, R. J.; Rashidi, M.; Seddon, K. R. *J. Chem. Soc., Dalton Trans.* **1978**, 1540–1544.

Scheme II

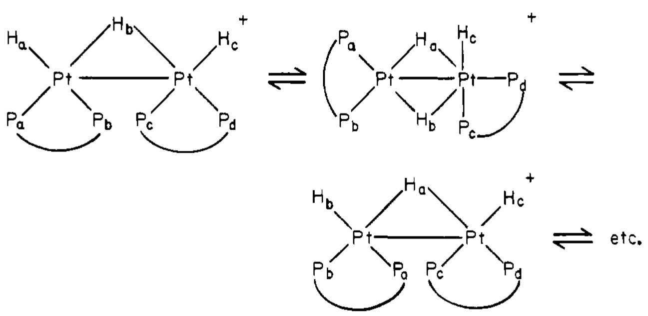

Recently an analogue of **1** exhibiting a cis–cis geometry about Pt has been prepared[2,29a] and characterized by X-ray diffraction.[29b] This complex, **11**, was originally thought to be a symmetrical dimer like **10**, and the terminal and bridging hydrides were found to be equivalent on the NMR time scale at −50 °C.[2] Contrast this behavior with that of **1**, which shows no evidence for bridge–terminal hydride exchange (by NMR) even at 100 °C in CD_3CN (in a sealed NMR tube).

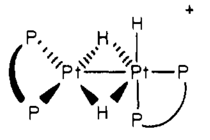

11, PP = bis(diphenylphosphino)ethane

The possibility of torsional nonrigidity in **1** should be acknowledged. Although it is not required by the NMR data, a process by which the entire *cis*-$Pt_A(H_b)_2(P_A)_2$ plane resolves around the Pt_A–Pt_B vector is fully consistent with the spectra and on this basis cannot be distinguished from rigid orthogonality of the two platinum coordination planes.[30]

Isoelectronic, 30-electron nickel,[8] rhodium,[9] and iridium[10] dimers containing two or more bridging hydride ligands have been structurally characterized. The neutral dimer $Ni_2(\mu\text{-}H)_2(\text{bisphos})_2$ (bisphos = $(c\text{-}Hx)_2P(CH_2)_3P(c\text{-}Hx)_2$) is formally a deprotonated analogue of **1** and **2**. The dimers $HL_2Rh(\mu\text{-}H)_3RhL_2$ (L = $P(i\text{-}Pr)_3$, $P(O\text{-}i\text{-}Pr)_3$) are 30-electron species; removal of a proton produces species with the same stoichiometry as **1** and **2**. In each case the MP_2 planes are approximately orthogonal, and the phosphine ligands occupy cis coordination sites about each metal atom.[8-10] Protonation of the rhodium complex when L = $P(O\text{-}i\text{-}Pr)_3$ yields[9] $HL_2Rh(\mu\text{-}H)_3RhL_2H^+$; an analogous iridium cation is known.[11]

It is interesting that platinum dimers such as **10** and **11** that contain chelating bis(phosphine) ligands undergo rapid interchange of bridging and terminal hydride ligands,[2,3] while **1** and **2** do not. This can be rationalized by considering the stereochemistry of the terminal and bridging hydrides about platinum. The bisphos ligands give rise to a cis–cis geometry for **10** and its congeners. As discussed above, this places each terminal hydride ligand cis to the $Pt(\mu\text{-}H)Pt$ bond. From this position, transient formation of a second hydride bridge could be facilitated; the intermediate thus produced is like **11**. This intermediate, in which the bridging hydride ligands are equivalent, could then revert back to its original geometry. Continually repeating the process, diagrammed in Scheme II, at each platinum will produce the averaged environment of hydride (and phosphorus as well) seen[2,3] in the NMR spectra of **10** and **11**. An intermediate having three bridging hydrides is also conceivable. Lack of fluxional exchange for **1** and **2** (and **7**[5] and **9**[1] as well) agrees with the geometries of these compounds, in which terminal hydride ligands occupy positions opposite the $Pt(\mu\text{-}H)Pt$ or $Pt(\mu\text{-}H)_2Pt$ bonds. The ability of these terminal hydrides to form a bridge to the distant platinum atom is thus severely hindered.

Spectral Parameters. The coupling constant between ^{195}Pt and an atom bound directly to it (e.g., P, H) tends to increase as the trans influence of the ligand trans to that atom decreases.[18] Since we have proposed **1**, **2**, and related dimers are composed of interlocking square-planar platinum(II) fragments, it is interesting to compare the values of the NMR parameters of these dimers to those found for mononuclear platinum(II) compounds. Values of the direct coupling constants between platinum and bridging hydrogen atoms, given in Table II, are smaller than values of $^1J_{PtH}$ for monomeric platinum(II) hydride complexes, which range from 700 to 1500 Hz.[18] The generally held assumption that coupling constants between directly bound atoms are dominated by the Fermi contact interaction leads to the prediction that values of $^1J_{AB}$ will be proportional to the valence s character of the bonding orbitals between atoms A and B.[18] The small values of $^1J_{PtH_b}$ in these dimers may reflect a reduction in the s character of the bonding orbitals due to rehybridization at platinum, as was suggested for dimer **9**.[1] Perhaps more important is the fact that the bonds between the bridging hydride ligands and platinum are electron deficient (three-center–two-electron for $Pt(\mu\text{-}H)Pt$ and four-center–four-electron for $Pt(\mu\text{-}H)_2Pt$). Thus the bonding electron density at each nucleus should be lower than in monomeric analogues. Two-bond couplings between the bridging hydride ligands and phosphorus atoms (Table II) are also lower than the corresponding values found for mononuclear analogues; e.g., for *cis*-**3** $^2J_{PH}{}^{trans} = 172$ Hz and $^2J_{PH}{}^{cis} = 24$ Hz, while for *trans*-**3** $^2J_{PH}{}^{cis} = 18$ Hz.[13a] These trends can be rationalized in a manner similar to that presented for $^1J_{PtH_b}$.

The value of $^1J_{Pt_AP_A} = 2741$ Hz for the *cis*-PtH_2P_2 moiety of **2** exceeds the corresponding value[12] of $^1J_{PtP} = 1984$ Hz for free *cis*-**3**. This indicates that the trans influence of the bridging hydrides (i.e., their σ-donor ability to Pt_A) is lower than that of the hydride ligands in *cis*-**3**, an observation consistent with the idea that electron density is donated by the *cis*-Pt_AH_2 moiety to *trans*-$Pt_BH(P_B)_2^+$ in the formation of **2**. Similarly, the value of the direct coupling constant between platinum and the terminal hydride ligands in **2** ($^1J_{PtH_t} = 1100$ Hz) is larger than the value of the corresponding coupling constant in *trans*-**3** ($^1J_{PtH} = 790$ Hz), consistent with the idea that the σ-donor ability (and hence trans influence) of the bridging hydride ligand is now divided between two metal centers. Recent work has demonstrated the ability of other cis hydrides such as $(\eta^5\text{-}C_5H_5)_2MoH_2$[31] and $IrH_2[P(i\text{-}Pr)_3]_2$[32] to donate to electron-deficient metal centers and thereby form dimers.

Reaction Chemistry. The results presented demonstrate that rapid, reversible formation of hydride-bridged cationic dimers is a general feature of the reactions of the sterically unhindered platinum(II) dihydride **3**. The common step in the formation of these dimers appears to be the very rapid displacement, by the PtH_2L_2 molecule, of a relatively weakly bound ligand X^- or S from *trans*-$PtHXL_2$ or *trans*-$PtH(S)L_2^+$. Such behavior

---

(29) (a) Minghetti, G.; Bandini, A. L.; Banditelli, G.; Bonati, F.; Szostak, R.; Knobler, C. B.; Kaesz, H. D., submitted for publication. (b) Minghetti, G.; Bandini, A. L.; Banditelli, G.; Boanti, F.; Knobler, C. B.; Kaesz, H. D., to be submitted for publication.

(30) Such torsional nonrigidity could in principle be detected by modifications of **1** that destroy the plane of symmetry that passes through the idealized $Pt_A(\mu\text{-}H)_2Pt$ plane. For example, the methyl groups of the dmpe ligand in $(dmpe)Pt(\mu\text{-}H)_2PtLL'H$ would be chemically inequivalent in a rigid geometry.

(31) Howarth, O. W.; McAteer, C. H.; Moore, P.; Morris, G. E.; Alcock, N. W. *J. Chem. Soc., Dalton Trans.* **1982**, 541–548.

(32) Musco, A.; Naegeli, R.; Venanzi, L. M.; Albinati, A. *J. Organomet. Chem.* **1982**, *228*, C15–C18.

was noted for formation of dimers such as **10** from the sterically hindered dihydrides *cis*-PtH_2(diphos).[3] It seems likely that the "hydride intermediate" (generated from $Pt(COD)_2$, L, and H_2) that reacted with *trans*-$PtH(S)L_2^+$ to yield analogues of **1** is also probably PtH_2L_2.[4] Reactions of **3** which generate species such as *trans*-$PtHXL_2$, where X^- can be displaced from platinum, immediately lead to dimer formation. We consider now the factors that control these reactions and that govern whether dimer **1** or dimer **2** is produced in a given reaction.

The solvent exerts a major control over the dimer-forming reactions of **3**, since nonpolar hydrocarbon solvents completely suppress the formation of dimeric cationic species, whereas polar solvents promote their formation. An illustration of this behavior is the reaction of **3** with carbon dioxide, which in toluene produces the insertion product **4** but in polar media yields $1^+HCO_2^-$. This solvent effect seems reasonable since the charged dimer and its counterion should be better solvated in polar media. Several factors will influence the equilibrium of dimer formation (eq 10). The enthalpy change will depend

$$PtH_2L_2 + trans\text{-}PtHXL_2 \rightleftharpoons Pt_2(\mu\text{-}H)_2HL_4^+ + X^- \quad (10)$$

on bond energies, solvation energies, and electrostatic energies due to ion-pair formation. Results of Yoshida et al. on the chemistry of *trans*-$PtH(OH)L_2$ (L = P(*i*-Pr)$_3$) indicate that in weak donor solvents (S = THF and H_2O) a significant amount of [*trans*-$PtH(S)L_2$][OH] forms.[25] It is at first surprising that such weakly basic solvents should displace hydroxide ion from platinum(II), but this may be explained if one assumes *solvation of the charged species is energetically favorable and drives the reaction.* Similar energetic factors may contribute to the negative enthalpy change (eq 10) when a dimer forms. Although the cis isomer of **3** is more favored in polar solvents (10% cis) than in hydrocarbon solvents (ca. 3% cis),[13a] we do not feel that this effect alone determines whether or not a dimer will be formed, since it appears that both isomers can react to produce a dimer (see below).

The equilibrium of eq 10 can be directly observed when X^- is iodide. When X^- is an oxygen donor anion such as OH^-, CH_3O^-, or HCO_2^-, the equilibrium lies far to the right in polar solvents, and no monomers can be detected by ^{31}P NMR spectroscopy; however, chemical evidence suggests eq 10 is reversible with these anions as well (see Results).[33] It is interesting that the reaction of **1** with CO results in phosphine redistribution whereas dimer **11**, which contains chelating phosphine ligands, produces $Pt_2(\mu\text{-}CO)(\mu\text{-}H)(dppe)_2^+$.[29b]

What determines whether dimer **1**, dimer **2**, or a mixture of **1** and **2** forms? To answer this question, we introduce the following hypothesis: dimer **1** forms when *cis*-PtH_2L_2 (*cis*-**3**) binds to the *trans*-$PtHL_2^+$ fragment, while dimer **2** forms when this fragment binds to *trans*-**3**. Several observations support this hypothesis. Both dimers can be formally broken down into *trans*-$PtHL_2^+$ and the respective isomer of **3** that we propose is the precursor to that dimer. The results of deuterium labeling show that, when **1** forms from PtD_2L_2 and *trans*-[$PtH(CD_3CN)L_2$][BF_4] (**5**), the two bridging positions are occupied by deuterium atoms while the hydrogen atom occupies only the terminal position. This result suggests that **1** forms from direct interaction of **5** with *cis*-**3**-d_2. An alternate possibility, that **2** first forms and then isomerizes to **1**, is unreasonable; since **2** is symmetrical, isomerization to **1** should result in some hydrogen in the bridging position. Below we consider in detail three reactions, in which either **1**, a mixture of **1** and **2**, or **2** alone initially forms. Our hypothesis about the precursor to each dimer provides a consistent rationalization of these results.

Methanol or water reacts with **3** at 25 °C to generate 1^+RO^- (R = CH_3, H). This reaction probably proceeds by slow formation of *trans*-$PtH(OR)L_2$, which then reacts with *cis*-**3** in a subsequent fast step (eq 11 and 12). Note that **2** could

$$PtH_2L_2 + ROH \xrightarrow{k_{11}} trans\text{-}PtH(OR)L_2 + H_2 \quad (11)$$

$$trans\text{-}PtH(OR)L_2 + cis\text{-}PtH_2L_2 \xrightarrow{k_{12}} 1^+RO^- \quad (12)$$

not be detected during the course of these reactions and that eq 12 is sufficiently rapid relative to eq 11 that no *trans*-$PtH(OR)L_2$ can be observed in the presence of **3**. Cis–trans isomerization of **3** is also fast relative to the process given by eq 11. Since eq 11 is the rate-determining step, *trans*-PH(OR)L_2 always forms in the presence of an excess of both *cis*- and *trans*-**3**. Furthermore, rapid isomerization assures the ratio [*cis*-**3**]/[*trans*-**3**] will remain approximately 0.1–0.2. If our hypothesis above is correct, **1** forms by selective reaction of the cis isomer of **3**, even though it is the minor form. This seems reasonable; **1** was shown to be more stable than **2**, which means *cis*-**3** binds more strongly to *trans*-$PtHL_2^+$ than does *trans*-**3**. Furthermore, steric considerations favor the reaction of *cis*-**3** since the *cis*-PtH_2 moiety is less hindered than the Pt–H moiety of *trans*-**3**. Initial formation of *trans*-$PtH(OR)L_2$ or [*trans*-$PtH(S)L_2$][RO] probably results from oxidative addition to or protonation of **3** to give the platinum(IV) intermediates $PtH_3(OR)L_2$ or [$PtH_3(S)L_2$][RO], followed by reductive elimination of H_2. Evidence of platinum(IV) intermediates in similar reactions of **3** was described elsewhere.[13a]

In the reaction between **3** and formic acid, a mixture of **1** and **2** appears initially, but **2** subsequently isomerizes completely to **1**. The reaction of **3** with formic acid proceeds much faster than with methanol or water. These rates correlate with the higher acidity of formic acid relative to methanol and water. The initial step in the formic acid reaction should be formation of **4** or **5** in a manner analogous to that suggested for methanol and water. Production of both **1** and **2** can be rationalized by assuming the reaction of **3** with HCO_2H forms **4** or **5** rapidly enough that these species react with *both* isomers of **3** before isomerization of *trans*-**3** to *cis*-**3** can occur. In fact, the initial ^{31}P NMR spectra of this reaction mixture show **1**, **2**, and **5** form initially. This implies that, when ROH = HCO_2H, k_{11} is sufficiently large that eq 11 is no longer the rate-determining step and that significant amounts of **3** are consumed in eq 11 before it can react in eq 12 or 13. Con-

$$trans\text{-}PtH(OR)L_2 + trans\text{-}3 \rightarrow 2^+RO^- \quad (13)$$

sequently, the initial ratio [**2**]/[**1**] is kinetically determined. When equilibrium is established at longer times, **2** converts completely to **1**.

Dimer **2** was the exclusive product of one reaction, the decomposition of **6**. Prior to the observation of **6**, hydridoalkoxo complexes of platinum(II) had not been observed but were strongly implicated in the formation of platinum(II) dihydrides by dehydrogenation of alcohols.[14] A key step in this process is assumed to be β-hydrogen transfer from the alkoxo ligand to platinum, accompanied by loss of aldehyde. Dimer **2** could form by the slow stereospecific production of *trans*-**3** from **6**, followed by the rapid reaction of *trans*-**3** with excess **6** to give **2** before any isomerization of *trans*-**3** occurs. Isomerization of $2^+CH_3O^-$ to **1** is slow in these solutions but accelerates upon warming.[34] We also observe that $2^+BPh_4^-$ in acetone solution does not isomerize to **1**, even after heating;

---

(33) It is interesting to contrast the role of dimer cleavage in the reactions of $Pt_2(\mu\text{-}H)_2HL_4^+$ systems with the lack of such equilibria in related $Rh_2(\mu\text{-}H)_3HL_4$ chemistry: Muetterties, E. L. *Inorg. Chim. Acta* **1981**, *50*, 1–9.

(34) Because these solutions contained CO_2 from the photochemical synthesis (see Experimental Section), the equilibrium $CH_3O^- + CO_2 \rightleftharpoons CH_3CO_3^-$ also should be considered.

however, addition of less than 1 equiv of iodide ion leads to rapid, complete isomerization of **2** to **1**, while an excess of pyridine causes slower isomerization.

Experimental Section

Materials. Solvents were deaerated prior to use by purging with nitrogen or an appropriate reactant gas or by several freeze–pump–thaw cycles on a high-vacuum line. High-purity acetonitrile and methanol (Burdick and Jackson) were used as received and stored under nitrogen. Benzene and tetrahydrofuran (Aldrich; reagent grade) were distilled under nitrogen from sodium/benzophenone. Benzene-d_6 (Merck) and toluene-d_8 (Aldrich) were dried over sodium/benzophenone and lithium aluminum hydride, respectively, and trap-to-trap distilled on a high-vacuum line. Acetonitrile-d_3 and acetone-d_6 (Merck) were used as received under nitrogen. The following gases were purchased from Matheson: hydrogen (99.999%), ethylene (CP), carbon monoxide (CP), deuterium (CP, 99% D), and carbon dioxide (Bone Dry). Isotopically enriched $^{13}CO_2$ (90% ^{13}C) was obtained from Merck & Co. A solution of sodium methoxide in methanol was prepared under nitrogen by careful addition of sodium to cold methanol. The following compounds were used without further purification: $NaBPh_4$ (Alfa, 99%), $LiBF_4$ (Alfa, 98%), [(n-Bu)$_4$N][I] (Aldrich, 98%), and $AgBF_4$ (Aldrich, handled under dry nitrogen and protected from light). $Pt(C_2O_4)(PEt_3)_2$,[13a] $PtH_2(PEt_3)_2$,[12] and *trans*-$PtHCl(PEt_3)_2$[35] were prepared by previously reported methods.

Spectra. IR spectra were recorded on a Perkin-Elmer 283 infrared spectrometer. Solution spectra were recorded in matched 0.1-mm CaF_2 or NaCl cells. Fourier transform NMR spectra were obtained on a JEOL FX90Q (^1H 89.6 MHz, ^{31}P 36.3 MHz, ^{195}Pt 19.2 MHz) or a JEOL FX270 spectrometer (^1H 296.7 MHz, ^{31}P 109.2 MHz). The notation $\{^1H\}$ indicates broad-band noise decoupling of the hydrogen nuclei. While the ^{31}P spectra were observed, selective decoupling of hydrogen nuclei at the resonance frequency of the triethylphosphine protons was done at low decoupler power and this allowed observation of splittings of phosphine resonances by hydride ligands. In general, pulse parameters were chosen to prevent saturation effects and ensure accurate integration of the NMR spectra. In some cases a software-controlled gated-pulse sequence that suppressed nuclear Overhauser enhancement (NOE) in $^{31}P\{^1H\}$ NMR spectra was used to enhance integration accuracy. All chemical shifts are positive in the direction of increasing frequency. ^1H chemical shifts were measured with use of the solvent resonance (arising from incomplete deuteration) relative to Me_4Si at 0 ppm; ^{31}P chemical shifts were measured relative to the deuterium resonance of the solvent with use of the internal frequency lock of the spectrometer and were assigned in such a way that the resonance from a capillary of 85% H_3PO_4 centered in a 10-mm NMR tube containing that deuterated solvent appeared at 0 ppm at 30 °C. (No corrections were made for spectra recorded at other temperatures.)

Spectral Simulation. Computer simulation of NMR spectra was performed with use of two programs. The program provided with the JEOL spectrometers was used to simulate the $^{31}P\{^1H\}$ and $^{195}Pt\{^1H\}$ NMR spectra. The large chemical shift difference between ^{31}P and ^{195}Pt was satisfactorily approximated by using a frequency separation of 0.9 MHz; smaller separations produced a distinct "leaning" of the ^{31}P and ^{195}Pt spectra toward each other. The program SIMEQ, provided for the Varian CFT-20 NMR spectrometer, was used to simulate the hydride portions of the ^1H NMR spectra. The chemical shift difference between ^1H and ^{31}P was satisfactorily modeled with use of a frequency separation of approximately 30 KHz. This program was able to treat couplings to a single ^{195}Pt nucleus by using the X approximation.[17]

General Procedures. Unless otherwise noted, all reactions were performed under oxygen-free conditions. Reactions to be monitored by NMR spectroscopy were conducted in 10-mm NMR tubes sealed with septum caps and flushed with nitrogen or an appropriate reactant gas. In some cases NMR tubes were blown onto ground-glass joints, manipulated, and sealed on a high-vacuum line. Partial pressures of gases were such that the total pressure above a solution was generally slightly greater than 1 atm. Unless otherwise noted, all reactions were conducted at ambient temperatures. In those reactions where dimers **1** or **2** were not isolated, their presence in solution was established by their characteristic $^{31}P\{^1H\}$ NMR spectra. Microanalyses were performed by Galbraith Laboratories, Knoxville, TN.

Photochemical Preparation of [$Pt_2(\mu\text{-}H)_2H(PEt_3)_4$][X], X = HCO_2^-, BPh_4^-, BF_4^-. A deaerated solution of $Pt(C_2O_4)(PEt_3)_2$ (0.26 g, 0.50 mmol) in acetonitrile (20 mL) under 1 atm of hydrogen was irradiated in a Schlenk tube with quartz walls with the output of a 450-W Hanovia mercury-arc lamp enclosed in a water-cooled quartz jacket. During irradiation, the Schlenk tube was connected to a mineral oil bubbler to release the pressure as CO_2 evolved, and a slow flow of H_2 was maintained over the solution, which was stirred magnetically. Heat generated by the irradiation must be dissipated either by directing a stream of cool air onto the Schlenk tube or by immersing the assembly in a bath of ice water; if this was not done, the solution darkened and some decomposition occurred. During irradiation, the solution gradually turned from colorless to orange and remained clear. The progress of the photoreaction could be followed by monitoring either the disappearance of the oxalate IR band of $Pt(C_2O_4)(PEt_3)_2$ at 1705 cm^{-1} or the $^{31}P\{^1H\}$ NMR spectrum. Irradiation was stopped at 80–90% conversion of the oxalate; further conversion is slow because the product absorbs most of the light. The spectra show that the oxalate complex that has photolyzed has been converted to **1**$^+HCO_2^-$ (Tables I and II; ^1H NMR HCO_2^- δ 8.54). This compound is not isolated; it does not crystallize upon cooling, and removal of the solvent under vacuum causes decomposition to a dark reddish brown, oily residue containing $Pt(PEt_3)_3$ (identified by comparison of its $^{31}P\{^1H\}$ NMR spectrum with that of an authentic sample) and finely divided platinum metal. Addition of $LiBF_4$ to **1**$^+HCO_2^-$ in solution yielded a precipitate of $LiHCO_2$, identified by comparison of its IR spectrum (Nujol) with that of an authentic sample. Removal of the solvent under vacuum produces **1**$^+BF_4^-$ as an air-stable, dark red-brown oil (IR (film) ν_{PtH_t} = 2155 s cm^{-1}, ν_{PtH_bPt} = 1648 w, br cm^{-1}), which could not be crystallized during several attempts. Addition of $NaBPh_4$ to a solution of **1**$^+HCO_2^-$ produced a precipitate of $NaHCO_2$, which was removed by filtration. Removal of solvent yielded a red-brown residue, which was dissolved in a minimal amount of acetone. Addition of methanol and cooling (−10 °C, 48 h) produced yellow crystals of bis(μ-hydro)*trans*-hydrotetrakis(triethylphosphine)diplatinum(II) tetraphenylborate, **1**$^+BPh_4^-$ (0.18 g, 0.15 mmol, 61%). Anal. Calcd: C, 48.65; H, 7.06; P, 10.45; Pt, 32.92; B, 0.93. Found: C, 48.90; H, 7.01; P, 10.48; Pt, 32.68; B (by difference), 0.91. These crystals were indefinitely air stable but hygroscopic. IR (Nujol): ν_{PtH_t} = 2150 s cm^{-1}, ν_{PtH_bPt} = 1655 br cm^{-1}.

NMR Studies of the Formation of 1 from $PtH_2(PEt_3)_2$ (3). A solution of **3** (20–40 mg, 3.5–7 mmol) in a given solvent (2–4 mL) was prepared under H_2 in a 10-mm NMR tube either by dissolving crystalline *trans*-**3**[13] or by generating **3** in situ by bubbling a stream of H_2 through a solution of $Pt(C_2H_4)(PEt_3)_2$.[12] The appropriate reagent was then added and the reaction followed by $^{31}P\{^1H\}$ NMR spectroscopy at or below ambient temperatures. Specific details follow.

a. Reaction of 3 with CO_2. Introduction of CO_2 to a solution of **3** in toluene-d_8 produced **4**, identified by its spectral parameters (see Results), in equilibrium with **3**. The reversibility of the formation of **4** was demonstrated by purging the solution with N_2 for 5 min and recording the ^{31}P NMR spectrum, which showed partial reversion of **4** to **3**. Purging with CO_2 again increased the amount of **4**. Integration of the ^{31}P NMR signals of an equilibrium mixture under ca. 1 atm of CO_2 shows the ratio [**4**]/[**3**] is approximately 2 at 0 °C. After addition of an equal volume of CH_3CN or THF, complete conversion to **1** occurred. Addition of CO_2 to a solution of **3** in acetonitrile or acetone yields only **1** immediately after mixing. Purging the acetone solution with a slow stream of hydrogen over several hours gradually converted **1**$^+HCO_2^-$ back to **3**.

b. Reaction of 3 with CH_3OH. When **3** was dissolved in CH_3OH, or when an equal volume of CH_3OH was added to a solution of **3** in toluene, **1** formed over a period of approximately 15 min. No intermediate compounds could be seen in the ^{31}P NMR spectra. It was not possible to verify the presence of the methoxide counterion by ^1H NMR methods because of interference by the large methanol resonance. Removal of the solvent under vacuum at 30 °C produced a dark red-brown oily residue, which was completely extracted into toluene-d_8. The NMR spectrum of this dark red-brown solution showed only $Pt(PEt_3)_3$.

c. Reaction of 3 with H_2O. This reaction, in CH_3CN solution, proceeded in a manner analogous to the reaction with methanol. The hydroxide counterion could not be directly observed, and removal of the solvent yielded $Pt(PEt_3)_3$ and platinum metal as in part b. Indirect evidence of hydroxide ion came from the observation that the product

---

(35) Parshall, G. W. *Inorg. Synth.* **1970**, *12*, 26–33. Chatt, J.; Duncanson, L. A.; Shaw, B. L. *Proc. Chem. Soc., London* **1957**, 343.

Table III. NMR Data for the Compounds [*trans*-$PtH(S)(PEt_3)_2$][BF_4]

	^{31}P NMR		^{1}H NMR, Pt-H			
S	chem shift, ppm[a]	$^{1}J_{PtP}$, Hz	chem shift, ppm[b]	$^{1}J_{PtH}$, Hz	$^{2}J_{PH}$, Hz	solvent
acetone-d_6	26.3	2696	−24.78	1484	14.7	acetone-d_6[c]
CD_3CN	22.1	2593	−17.71	1231	14	CD_3CN[d]
MeOH	27.4	2704	*e*	*e*	*e*	$MeOH/C_6D_6$[c]
pyridine	20.2	2636	*e*	*e*	*e*	$MeOH/C_6D_6$[c]

[a] Singlet with ^{195}Pt satellites. [b] 1:2:1 triplet with ^{195}Pt satellites. [c] 30 °C. [d] 20 °C. [e] Not recorded.

catalyzed the addition of H_2O to CH_3CN to give $CH_3C(O)NH_2$, which was separated from the reaction mixture by removing the solvent and subliming $CH_3C(O)NH_2$ from the residue; identification was by comparison of ^{1}H NMR and IR spectra with those of an authentic sample. Addition of $[Et_4N][OH]$ (0.15 mmol) to a mixture of CH_3CN (12 mmol) and H_2O (3.4 mmol) also catalyzed the formation of $CH_3C(O)NH_2$.

d. Reaction of 3 with HCO_2H. Formic acid (95–97%) (2 mL) was added to a solution of **3** in acetone-d_6 (0.5 mL), and the solution was immediately transferred to the NMR spectrometer probe at 0 °C. The $^{31}P\{^{1}H\}$ NMR spectrum revealed a mixture of **1**, **2**, and **5** (identified by its NMR parameters—see below and Table III). Further interconversions among these products could be observed by briefly warming to ambient temperature and then cooling again and recording the spectrum.

e. Preparation of 1-d_2 from 3-d_2 and *trans*-$PtH(S)L_2^+$ (5), S = CD_3CN. To a CD_3CN solution of **5** (prepared as described below) was added an equimolar amount of $Pt(C_2H_4)(PEt_3)_2$ in CD_3CN. These species did not react as seen by the $^{31}P\{^{1}H\}$ NMR spectrum. This solution was purged with D_2 at 25 °C for 2 min to convert the ethylene complex to **3**-d_2, and the ^{1}H NMR spectrum of the solution was immediately recorded at −50 °C. Only the signal for terminal hydride of **1** could be detected; this appeared at δ −4.77 in precise agreement with the spectrum of **1**-d_0 in CD_3CN. From this it was concluded that $[Pt_2(\mu\text{-}D)_2HPEt_3)_4][BF_4]$ had formed.

Formation and Isolation of [$Pt_2(\mu\text{-}H)H_2(PEt_3)_4$][$BPh_4$] (2). Solutions of *trans*-$PtH(OCH_3)(PEt_3)_2$ (**6**) were prepared by UV irradiation of solutions of $Pt(C_2O_4)(PEt_3)_2$ in methanol or methanol/C_6D_6, as previously described.[12] While it stood in the dark at ambient temperature or after it was heated to 70 °C for 15 min, **6** converted cleanly to **2**. Complex **6** could also be prepared by addition of a solution of $NaOCH_3$ in methanol to a solution of [*trans*-$PtH(CH_3OH)(PEt_3)_2$][BF_4] (prepared as described below) in a mixture of methanol and C_6D_6 at −10 °C.[12] For unknown reasons (perhaps due to excess CH_3O^-) solutions of **6** prepared this way rapidly yielded **2** at 25 °C. Removal of the solvent under vacuum from solutions of **2** prepared by these routes caused the solutions to darken and led to decomposition. (μ-Hydro)-*trans*-dihydrotetrakis(triethylphosphine)diplatinum(II) tetraphenylborate, $\mathbf{2}^+BPh_4^-$, contaminated with $\mathbf{1}^+BPh_4^-$, was isolated as a yellow-brown solid by adding $NaBPh_4$ to a solution of **2** (prepared by the photochemical route), concentrating under vacuum, and cooling to −15 °C for 48 h. Starting with 0.50 g of $Pt(C_2O_4)(PEt_3)_2$ (0.96 mmol), 0.11 g of dimer salts (0.093 mmol, 19%) was obtained, of which roughly 65% was $\mathbf{2}^+BPh_4^-$. The infrared spectrum of a solution of this solid in CH_2Cl_2 contained signals that were assigned to **2** ($\nu_{PtH_t} = 2150$ s cm^{-1}, $\nu_{PtH_bPt} \approx 1640$ br cm^{-1}) along with the expected signals arising from **1**.

Reaction of 1 with I^-. As $[(n\text{-}Bu)_4N][I]$ in acetone-d_6 was added to a solution of $\mathbf{1}^+BPh_4^-$ in acetone-d_6, it was seen from the $^{31}P\{^{1}H\}$ NMR spectrum (109 MHz) that **1** was partially converted to **3** and *trans*-$PtHI(PEt_3)_2$. The approximate relative concentrations of I^- and **1** were determined by comparison of the areas of the $(n\text{-}Bu)_4N^+$ and PEt_3 resonances in the ^{1}H NMR spectra (270 MHz). Relative concentrations of the platinum species were obtained by integration of the $^{31}P\{^{1}H\}$ NMR spectra, and from these data an approximate value of K was calculated. It was further observed that K varied reproducibly with temperature between +30 and −30 °C; a plot of $\ln K$ vs. $1/T$ was a straight line and yielded approximate values of ΔH and ΔS.

Reaction of 1 with C_2H_4. A solution of $\mathbf{1}^+HCO_2^-$ in a mixture of CH_3CN and C_6D_6 was purged with C_2H_4 for 5 min and left in the dark at 30 °C. Periodic checks of the ^{31}P NMR spectrum over a 2-day period showed gradual clean conversion to $Pt(C_2H_4)(PEt_3)_2$. When this was repeated with $\mathbf{1}^+BPh_4^-$ instead, no reaction was detected.

Reaction of $\mathbf{1}^+HCO_2^-$ with $^{13}CO_2$. An NMR tube containing a solution of $\mathbf{1}^+HCO_2^-$ in CD_3CN was attached to a high-vacuum line, and a quantity of $^{13}CO_2$ (90% ^{13}C) sufficient to provide a partial pressure of approximately 1 atm was condensed into the tube with use of liquid nitrogen. The solution was warmed to 30 °C for 15 min, and then the ^{1}H NMR spectrum was recorded. The signal for $H^{12}CO_2^-$ was a singlet at δ 8.54, and a signal for $H^{13}CO_2^-$ appeared as a doublet centered around 8.54 ppm with a separation $^{1}J_{^{13}CH} = 180$ Hz. The relative intensities of these signals indicated complete isotopic scrambling between ^{13}C and ^{12}C in the formate ion, on the basis of the relative amounts of $^{13}CO_2$ and $^{12}CO_2$ present.

Catalytic Decomposition of HCO_2H. The catalytic decomposition of HCO_2H to H_2 and CO_2 was monitored by measuring the change in pressure above stirred and thermostated solutions that were connected to a vacuum line of known volume and shielded from room light. The pressure was measured with a mercury manometer, and the moles of gas evolved were calculated with use of the ideal-gas law; corrections were not made for dissolved gas, but these should be minimal since the gas volume (175 mL) was much larger than the liquid volume (5 mL). No gas evolved over 24 h from a solution of $\mathbf{1}^+BPh_4^-$ (32 mg, 0.027 mmol) in formic acid (3.0 mL, 76 mmol) and acetone-d_6 (1.4 mL) at 20.0 ± 0.3 °C. The $^{31}P\{^{1}H\}$ NMR spectrum of this solution after 24 h showed partial conversion of **1** to **5**. Addition of approximately 3 mmol of $NaHCO_2$ to the solution produced immediate and sustained gas evolution but no apparent change in the $^{31}P\{^{1}H\}$ NMR spectrum. Gas evolution was measured from a solution of **1** (0.038 mmol) in methanol (3.5 mL) containing HCO_2H (2.5 mL, 66 mmol) and NaO_2CH (7.6 mmol) thermostated at 20 ± 0.3 °C. Throughout these reactions the pale yellow solutions remained clear and homogeneous.

Isomerization of 2 to 1. A solution in acetone-d_6 of $\mathbf{2}^+BPh_4^-$, isolated as described above and contaminated with $\mathbf{1}^+BPh_4^-$, showed no isomerization after 1 h at 25 °C or after 15 min at 70 °C. Isomerization of **2** to **1** took place slowly (25 min at 70 °C) upon addition of excess pyridine and rapidly at 25 °C upon addition of less than 1 equiv (based on **2**) of $(n\text{-}Bu)_4N^+I^-$.

Preparation and Spectra of [*trans*-$PtH(S)(PEt_3)_2$][BF_4] (5), S = CD_3CN, $(CD_3)_2CO$, CH_3OH, Pyridine. Complexes **5** were generated in situ by treatment of *trans*-$PtHCl(PEt_3)_2$ with 1 equiv of $AgBF_4$ under nitrogen in the particular solvent, except for the complex with pyridine, which was prepared by adding pyridine to **5**, S = CH_3OH. After filtration to remove AgCl, $^{31}P\{^{1}H\}$ and ^{1}H NMR spectral parameters were recorded (Table III).

Acknowledgment. We thank the National Science Foundation (Grants CHE 78-01615 and 81-05069) for financial support, and Johnson Matthey, Inc., for a generous loan of platinum. We thank Professor Kaesz for sharing results[29] with us prior to their publication.

Registry No. $\mathbf{1}^+HCO_2^-$, 81800-04-6; $\mathbf{1}^+BPh_4$, 81800-05-7; $\mathbf{1}^+BF_4^-$, 69277-95-8; $\mathbf{1}^+HO^-$, 84680-52-4; $\mathbf{1}^+CH_3O^-$, 84680-53-5; **1**-d_2, 84624-77-1; **2**, 84624-72-6; *trans*-**3**, 62945-61-3; *cis*-**3**, 80581-70-0; **3**-d_2, 84624-78-2; **4**, 81768-78-7; **5** (S = $(CD_3)_2CO$), 84624-74-8; **5** (S = HCO_2H), 84624-75-9; **5** (S = CD_3CN), 84624-80-6; **5** (S = py), 84624-82-8; **6**, 81457-60-5; $Pt(C_2O_4)L_2$, 81457-59-2; *trans*-$PtH(CH_3OH)(PEt_3)_2$][BF_4], 84624-81-7; *trans*-$PtHI(PEt_3)_2$, 16971-06-5; $Pt(C_2H_4)(PEt_3)_2$, 76136-93-1; HCO_2H, 64-18-6; *trans*-$PtHCl(PEt_3)_2$, 16842-17-4; CH_3CN, 75-05-8; $CH_3C(O)NH_2$, 60-35-5.

Supplementary Material Available: Figures showing the outermost satellite signals of isotopomers **1ii**–**1iv** of $\mathbf{1}^+BPh_4^-$ and their computer simulations and the central multiplets of Figure 3 along with the computer simulation for **1i** (2 pages). Ordering information is given on any current masthead page.